

## Energy band structure of LaCuOCh (Ch = S, Se and Te) calculated by the full-potential linearized augmented plane-wave method

This article has been downloaded from IOPscience. Please scroll down to see the full text article.

2004 J. Phys.: Condens. Matter 16 5179

(<http://iopscience.iop.org/0953-8984/16/28/036>)

View [the table of contents for this issue](#), or go to the [journal homepage](#) for more

Download details:

IP Address: 129.252.86.83

The article was downloaded on 27/05/2010 at 16:02

Please note that [terms and conditions apply](#).

# Energy band structure of LaCuOCh (Ch = S, Se and Te) calculated by the full-potential linearized augmented plane-wave method

Kazushige Ueda<sup>1,2,5</sup>, Hideo Hosono<sup>2,3</sup> and Noriaki Hamada<sup>4</sup>

<sup>1</sup> Department of Materials Science, Faculty of Engineering, Kyushu Institute of Technology, 1-1 Sensui, Tobata, Kitakyushu 804-8550, Japan

<sup>2</sup> Hosono Transparent Electro-Active Materials (TEAM) Project, ERATO, Japan Science and Technology Agency, KSP C-1232, 3-2-1 Sakado, Takatsu, Kawasaki 213-0012, Japan

<sup>3</sup> Materials and Structures Laboratory, Tokyo Institute of Technology, 4259 Nagatsuta, Midori, Yokohama 226-8503, Japan

<sup>4</sup> Department of Physics, Faculty of Science and Technology, Tokyo University of Science, 2641 Yamazaki, Noda, Chiba 278-8510, Japan

E-mail: [kueda@che.kyutech.ac.jp](mailto:kueda@che.kyutech.ac.jp)

Received 25 February 2004

Published 2 July 2004

Online at [stacks.iop.org/JPhysCM/16/5179](http://stacks.iop.org/JPhysCM/16/5179)

doi:10.1088/0953-8984/16/28/036

## Abstract

Energy band diagrams of LaCuOCh (Ch = S, Se and Te) were calculated by a full-potential linearized augmented plane-wave method. The calculations, based on the local density approximation with/without an on-site Coulomb repulsion parameter, were to examine the energy levels of La 4f states. The results of the calculations showed that the on-site correlation parameter is necessary for evaluating the energy levels of La 4f states appropriately. The calculations for LaCuOCh with the on-site correlation parameter revealed that LaCuOS and LaCuOSe have almost the same energy band structure with a direct allowed-type band gap, while LaCuOTe has significantly different conduction band structure that exhibits an indirect-type band gap. This difference in electronic structure between LaCuOCh (Ch = S, Se and Te) is consistent with the observed optical properties of these materials.

## 1. Introduction

LaCuOCh (Ch = S, Se and Te) is a layered material consisting of  $(\text{La}_2\text{O}_2)^{2+}$  and  $(\text{Cu}_2\text{Ch}_2)^{2-}$  layers stacked along the *c*-axis [1–3]. Since its layered structure is similar to that of Cu-based high- $T_c$  superconducting oxides, the electrical transport properties of LaCuOS and LaCuOSe were examined in detail at low temperatures [4, 5]. In addition to the electrical transport

<sup>5</sup> Author to whom any correspondence should be addressed.

properties, thermoelectric properties have also been investigated at high temperatures [6, 7]. Recently, transparent and excitonic emission/absorption features were found in LaCuOS through research on transparent p-type conducting oxides [8, 9]. Because these optical features, as well as p-type conductivity, are very attractive for optoelectronic applications of these materials, various studies on optical and electrical properties [10–14], electronic structures [15, 16] and film growth techniques [17–19] have been undertaken by several researchers.

The electronic structure of LaCuOS was previously analysed using an energy band calculation and photoemission spectroscopy in order to understand its fundamental physical properties [15]. However, the previous band calculation did not include unoccupied La 4f states. Recently, the optical and electrical properties of several analogous materials, with the formula  $\text{LnCuOCh}$  ( $\text{Ln} = \text{La, Ce, Pr and Nd}$ ;  $\text{Ch} = \text{S, Se}$ ), were reported [20, 21, 12], and  $\text{LnCuOTe}$  ( $\text{Ln} = \text{La, Ce, Pr and Nd}$ ) was synthesized providing a variation on the materials in the  $\text{LnCuOCh}$  system [3, 22]. Although LaCuOS is a prototype material in the  $\text{LnCuOCh}$  system, its electronic structure does not always represent those of other materials in the system. For instance, a unique electronic structure of CeCuOS was observed by photoemission spectroscopy, as well as its unique crystal structure [20, 21]. In this study, the electronic structures of  $\text{LaCuOCh}$  ( $\text{Ch} = \text{S, Se and Te}$ ) are calculated, including the La 4f states, by means of the local density approximation (LDA) or the LDA with an on-site Coulomb repulsion parameter,  $U$ , (LDA +  $U$ ), and the differences in their electronic structures along with experimental observations discussed.

## 2. Experiments

### 2.1. Energy band calculations

The electronic structure of  $\text{LaCuOCh}$  ( $\text{Ch} = \text{S, Se and Te}$ ) was calculated by the ABCAP code [23]<sup>6</sup> in a full-potential linearized augmented plane-wave (FLAPW) method. The parameters for their crystal structures were taken from [24] for LaCuOS and LaCuOSe, and from [3] for LaCuOTe. Each crystal structure belongs to the tetragonal system with the space group of  $P4/nmm$ . The muffin-tin radii used in the calculations were set to 2.7 au for La, 2.1 for Cu, 1.4 for O, 1.9 for S, 2.0 for Se and 2.0 for Te. The calculations were iterated self-consistently until the total electron energy of the crystals converged to less than 0.1 mRyd.

The FLAPW calculations based on density functional theory were performed basically within the framework of the LDA. Three different calculations were made to evaluate the energy levels of La 4f states and the influence of on-site correlation parameters; calculations (I) without La 4f states using the LDA, (II) with La 4f states using the LDA and (III) with La 4f states using the LDA +  $U$ . The empirical parameters for the La 4f states used in the LDA +  $U$  calculations were fixed at 11.0 eV for the on-site Coulomb parameter  $U$  and 0.36 eV for the on-site exchange parameter  $J$  [25].

### 2.2. Spectral measurements

Photoemission spectroscopy (PES) and inverse photoemission spectroscopy (IPES) measurements were carried out using densely sintered discs as samples. UV light from a He discharge lamp was used in the PES measurements and UV photons emitted from samples were detected in the IPES measurements. The details of the measurements were reported in

<sup>6</sup> ABCAP (the all-electron band-structure calculation package) in the ‘Frontier Simulation Software for Industrial Science (FSIS)’ Project, MEXT, Japan.

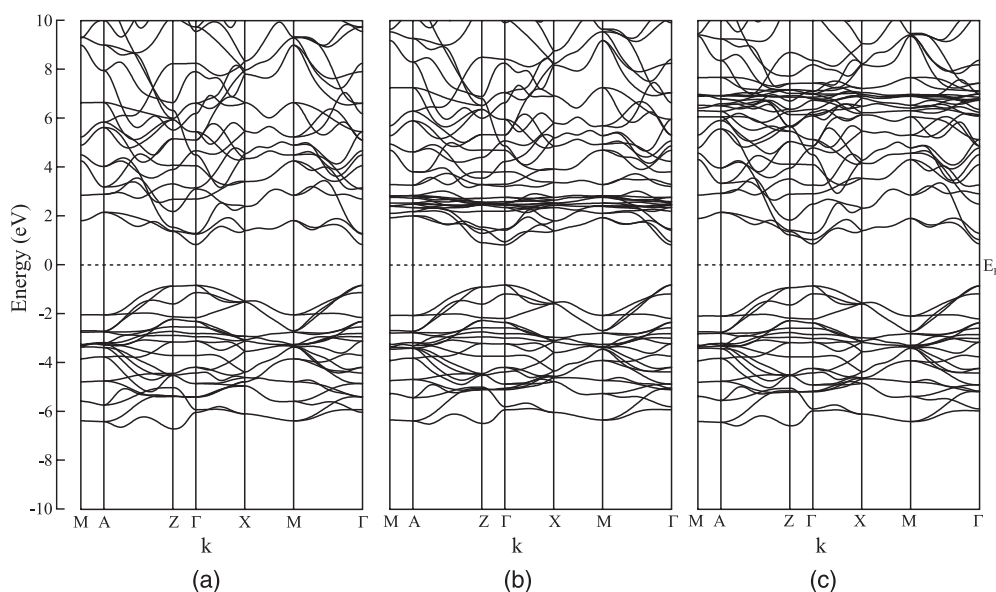


**Figure 1.** Energy band diagrams of LaCuOS calculated using (a) the LDA without La 4f states, (b) the LDA with La 4f states and (c) the LDA +  $U$  with La 4f states.

the previous paper [15]. Diffuse reflection spectra of powder samples and PL spectra of disc samples were measured at room temperature. Conventional UV–visible spectrometers were used in the diffuse reflection measurements. In the PL measurements,  $4\omega$  from a YAG:Nd laser was used for photo-excitation along with a CCD detector. The single-phase samples for these measurements were prepared by solid state reaction in evacuated silica tubes at high temperatures. The details of the sample preparation were described elsewhere [10, 3].

### 3. Results and discussion

#### 3.1. Energy band structure

Energy band diagrams of LaCuOS evaluated in the three different calculations are shown in figure 1. Figure 1(a) shows the band diagram without La 4f states, which is the same as that reported in our previous paper [15]. Since the La 4f states are not taken into account in calculation (I), the band structure in the conduction band is fairly simple. On the other hand, in figures 1(b) and (c), low dispersion states originating from the La 4f states appear in the conduction band. Although both calculations, (II) and (III), include the La 4f states, the energy positions of the 4f states differ considerably; the energies are approximately 3 eV above the Fermi energy for calculation (II) and 7 eV for calculation (III). This difference arises from the on-site Coulomb repulsion of La 4f electrons, and very similar results are obtained in the band calculations of  $\text{La}_2\text{CuO}_4$  using the local spin density approximation (LSDA) and LSDA +  $U$  [24].

Unoccupied La 4f states are usually located several electronvolts higher than the Fermi energy, according to IPES spectra for some La containing materials: at 5–6 eV for La metal and 8–9 eV for  $\text{La}_2\text{CuO}_4$  [26–29]. The total density of states (DOS) and partial DOSs (PDOSs) evaluated in calculation (III) are shown in figure 2. La 4f states concentrated at around 7 eV are seen above broad La 5d states in the conduction band. It is, therefore, considered that the

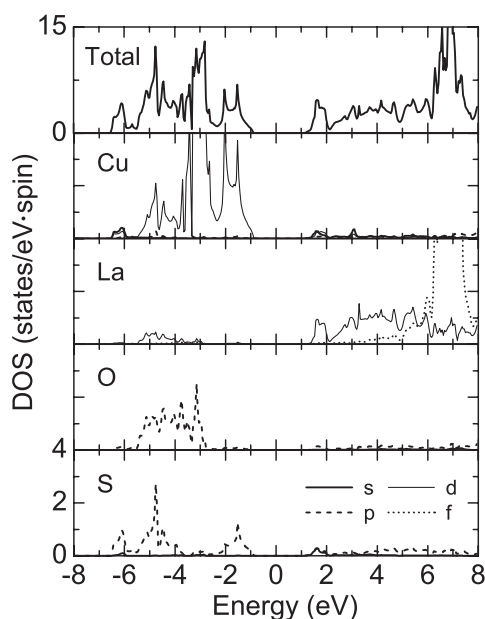


**Figure 2.** The total DOS and PDOSs of LaCuOS estimated using the LDA +  $U$  with La 4f states.

calculation (III) based on the LDA +  $U$  gives more reasonable results than the calculation (II) as regards the La 4f states, and the on-site Coulomb repulsion parameter  $U$  is essential for the band calculation to evaluate the La 4f energy levels correctly.

As shown in figure 1, almost no discernible difference in the valence band structure is seen irrespective of the presence of the La 4f states. This is simply because the amount of PDOS of the La 4f states is negligible in the valence band. In addition to the valence band, the bottom of the conduction band is also little influenced by the 4f states, as seen by comparing figures 1(a) and (c). Since the La 4f states do not mix with either the valence or conduction bands near the energy gap, the symmetry of the conduction band minimum (CBM) ( $\Gamma_1^+$ ) and the valence band maximum (VBM) ( $\Gamma_5^-$ ) is the same in calculations (I) and (III).

Energy band diagrams of LaCuOCh (Ch = S, Se and Te) calculated by the LDA +  $U$  method are shown in figure 3. All the materials show very similar valence structures, but the top parts of the valence band (the top four states at  $\Gamma$  point), which are anti-bonding states composed of Cu 3d and chalcogen p states, slightly widen in the order LaCuOS, LaCuOSe and LaCuOTe. This widening indicates that the hybridization between the two states increases in the same order.

In the conduction band, LaCuOS and LaCuOSe show very similar structure and the La 4f states are located at almost the same energy level. Both the CBM and VBM of these materials are located at the  $\Gamma$  point and the symmetries of the two states are the same for them, indicating that LaCuOSe has a direct allowed band gap like LaCuOS. However, LaCuOTe shows a conduction band structure different from those of the other two materials. The remarkable difference is two minimum points in the conduction band near the M point, these components being primarily La 5d states rather than Cu 4s states. Since the energy level of these two minima is almost the same as that of the minimum at the  $\Gamma$  point, it is hard to determine whether this material has a direct or indirect band gap. (The calculation (I) without the La 4f states for LaCuOTe apparently gives an indirect band gap between the CBM near the M point and the VBM at the  $\Gamma$  point.) The calculated energy gaps are 1.75 eV for LaCuOS, 1.48 eV

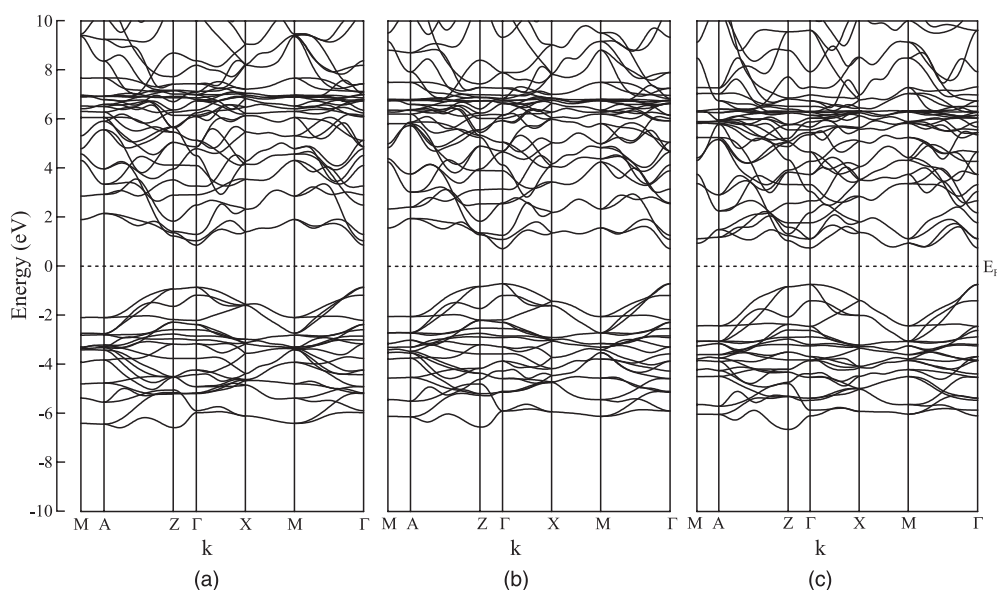


**Figure 3.** Energy band diagrams of LaCuOCh (Ch = S, Se and Te) calculated by the LDA +  $U$  method.

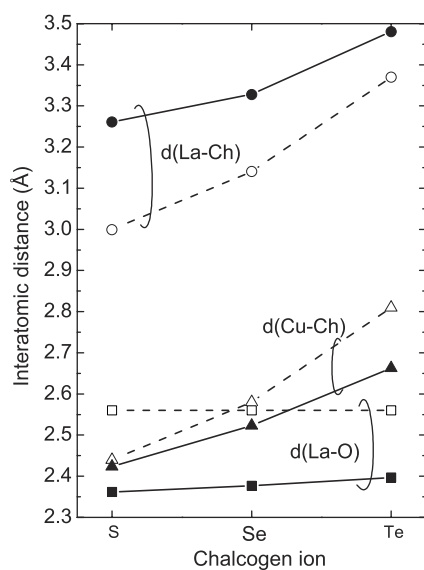


**Figure 4.** Interatomic distances (closed symbols) in LaCuOCh (Ch = S, Se and Te) along with the sum of the ionic radii of the ion pairs (open symbols): La–O (squares), La–Ch (circles) and Cu–Ch (triangles).

for LaCuOSe and 1.42 eV for LaCuOTe. Although these values are smaller than the observed energy gaps [10], 3.1 eV for LaCuOS, 2.8 eV for LaCuOSe and 2.2 eV for LaCuOTe, the band calculation was able to give the trend of their relative magnitudes.

Figure 4 shows interatomic distances in LaCuOCh estimated from the crystal structural data along with the sum of the ionic radii of ion pairs [30]. As discussed for the LnCuOS

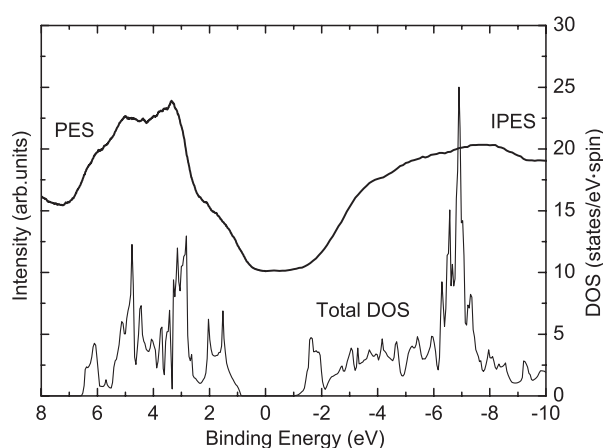


Figure 5. PES and IPES spectra of LaCuOS along with its total DOS.

(Ln = La, Ce, Pr and Nd) system [21], the La–O distance is much shorter or the La–Ch distance is much longer than the sum of these ionic radii due to the layered structure of these compounds. The deviation of the Cu–Ch distance from the sum of the ionic radii increases in the order S, Se and Te, decreasing the Cu–Ch distance. The decrease in the Cu–Ch distance indicates increase of the covalency in the Cu–Ch bond. It is noteworthy that the La–Ch distance also decreases in comparison with the sum of the ionic radii in a similar manner to the Cu–Ch distance. This decrease in the La–Ch distance suggests that the interactions between the La and Ch ions, which are interlayer interactions, increase as the chalcogen ions become heavier, and the La–Te interactions are larger than the other La–Ch interactions. It is, therefore, supposed that the increase in the La–Te interactions is responsible for the indirect band gap feature of LaCuOTe.

### 3.2. Comparison with photoemission spectra

PES and IPES spectra of LaCuOS are shown along with the total DOS in figure 5. The relative intensity of the PES and IPES spectra was arbitrarily scaled for comparison with the calculated DOS. The energy scale of the PES and IPES spectra was calibrated using the Fermi energy of Au metal. The energy of the VBM in the PES spectrum is close to the Fermi energy ( $E = 0$  eV), which demonstrates that the LaCuOS sample is a p-type conductive material.

The calculated total DOS in the valence band remains almost unchanged from that in the previous report. In contrast, the calculation in this study gives an intense DOS assignable to La 4f states at  $-7$  eV in the conduction band. The IPES spectrum shows two broad bands around  $-4$  and  $-8$  eV, and both of them were assigned to La 5d states in our previous study [15]. However, the present LDA +  $U$  calculation reveals that the broad band at around  $-8$  eV should be assigned to the La 4f states rather than the La 5d states. This assignment to the La 4f states is reasonable in comparison with the conduction band structure of other La containing materials such as La metal and La<sub>2</sub>CuO<sub>4</sub>. The low intensity of the 4f states is due to the low ionization cross-section of the La 4f states for UV excitation in the IPES measurements [31]. A small intensity of the La 4f states measured by UV IPES is frequently observed for the La containing materials in comparison with x-ray IPES spectra [26–29].

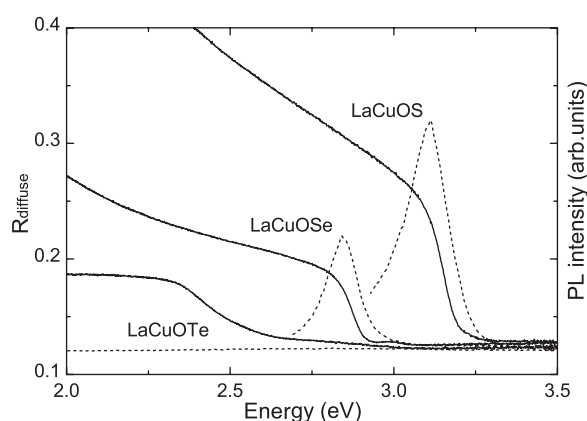


**Figure 6.** Diffuse reflection spectra (solid curve) and PL spectra (dashed curve) of LaCuOCh (Ch = S, Se and Te).

### 3.3. Diffuse reflection and PL spectra

Figure 6 shows diffuse reflection spectra and PL spectra of LaCuOCh (Ch = S, Se and Te) at room temperature. As reported in our previous paper [10], LaCuOS and LaCuOSe show a relatively sharp diffuse reflection drop at the absorption edge. Corresponding to the sharp diffuse reflection drop, intense photoluminescence is observed in these materials. These results are consistent with the calculated energy band structure, indicating that the energy gap of LaCuOS and LaCuOSe is of direct allowed type.

The diffuse reflection of LaCuOTe gradually decreases around 2.4 eV, and the diffuse reflection drop is not as sharp as those for LaCuOS and LaCuOSe. In addition, no photoluminescence peak was observed in the present study. The absence of the sharp diffuse reflection drop and photoluminescence suggests that the energy gap of LaCuOTe is of indirect type in contrast to those of the other two materials, although the type of the energy gap is not determined clearly from the energy band diagram of LaCuOTe. Results of both optical measurements and energy band calculations demonstrate that the band structure of LaCuOTe is significantly different from those of LaCuOS and LaCuOSe.

## 4. Conclusions

Energy band calculations were carried out by the FLAPW method to examine the energy band structures of LaCuOCh (Ch = S, Se and Te) including the La 4f states. The calculation using the standard LDA estimates energies of the La 4f states much lower than the experimental results, while the calculation using the LDA +  $U$  provides reasonable energies for the La 4f states. Therefore, it becomes clear that the LDA +  $U$  calculation is essential for evaluating the La 4f states appropriately. On the basis of the energy band diagram including the La 4f states, the peak at approximately 8 eV above the Fermi energy observed in the IPES spectrum was assigned to the La 4f states.

A series of the band calculations for LaCuOCh (Ch = S, Se and Te) reveals that LaCuOS and LaCuOSe have very similar energy band structures and a direct-type energy gap at the  $\Gamma$  point. On the other hand, LaCuOTe has different energy band structure, especially in the conduction band, and its energy gap is of indirect type. The presence of the sharp diffuse reflection drop and photoluminescence at the absorption edge in LaCuOS and LaCuOSe,



as well as their absence in LaCuOTe, experimentally support the differences in calculated band structure between the LaCuOCh (Ch = S, Se and Te) compounds.

## References

- [1] Palazzi M 1981 *C. R. Acad. Sci.* **292** 789
- [2] Zhu W J, Huang Y Z, Dong C and Zhao Z X 1994 *Mater. Res. Bull.* **29** 143
- [3] Popovkin B A, Kusainova A M, Dolgikh V A and Aksel'rud G 1998 *Russ. J. Inorg. Chem.* **43** 1471
- [4] Takano Y, Yahagi K and Sekizawa K 1995 *Physica B* **206/207** 764
- [5] Ohtani T, Hirose M, Sato T, Nagaoka K and Iwabe M 1993 *Japan. J. Appl. Phys.* **32** (Suppl. 32–3) 316
- [6] Ishikawa K, Kinoshita S, Suzuki Y, Matsuura S, Nakanishi T, Aizawa M and Suzuki Y 1991 *J. Electrochem. Soc.* **138** 1166
- [7] Yasukawa M, Ueda K and Hosono H 2004 *J. Appl. Phys.* **95** 3594
- [8] Ueda K, Inoue S, Hirose S, Kawazoe H and Hosono H 2000 *Appl. Phys. Lett.* **77** 2701  
Ueda K, Inoue S, Hosono H, Sarukura N and Hirano M 2001 *Appl. Phys. Lett.* **78** 2333
- [9] Ueda K, Hiramatsu H, Ohta H, Hirano M, Kamiya T and Hosono H 2004 *Phys. Rev. B* **69** 155305
- [10] Ueda K and Hosono H 2002 *J. Appl. Phys.* **91** 4768
- [11] Hiramatsu H, Ueda K, Ohta H, Hirano M, Kamiya T and Hosono H 2003 *Appl. Phys. Lett.* **82** 1048
- [12] Hiramatsu H, Ueda K, Takafuji K, Ohta H, Mirano M, Kamiya T and Hosono H 2003 *J. Appl. Phys.* **94** 5805
- [13] Takase K, Koyano M, Shimizu T, Makihara K, Takahashi Y, Takano Y and Sekizawa K 2002 *Solid State Commun.* **123** 531
- [14] Kamioka H, Hiramatsu H, Ohta H, Hirano M, Ueda K, Kamiya T and Hosono H 2004 *Appl. Phys. Lett.* **84** 879
- [15] Inoue S, Ueda K, Hosono H and Hamada N 2001 *Phys. Rev. B* **64** 245211
- [16] Sato H, Negishi H, Wada A, Ino A, Negishi S, Hirai C, Namatame H, Taniguchi M, Takase K, Takahashi Y, Shimizu T, Takano Y and Sekizawa K 2003 *Phys. Rev. B* **68** 035112
- [17] Hiramatsu H, Ueda K, Ohta H, Orita M, Hirano M and Hosono H 2002 *Thin Solid Films* **411** 125
- [18] Hiramatsu H, Ueda K, Ohta H, Orita M, Hirano M and Hosono H 2002 *Appl. Phys. Lett.* **81** 598
- [19] Hiramatsu H, Ohta H, Suzuki T, Honjo C, Ikuhara Y, Ueda K, Kamiya T, Hirano M and Hosono H 2004 *Cryst. Growth Des.* **4** 301
- [20] Ueda K, Takafuji K, Hiramatsu H, Ohta H, Kamiya T, Hirano M and Hosono H 2003 *Chem. Mater.* **15** 3692
- [21] Ueda K, Takafuji K and Hosono H 2003 *J. Solid State Chem.* **170** 182
- [22] Charkin D O, Akopyan A V and Dolgikh V A 1999 *Russ. J. Inorg. Chem.* **44** 833
- [23] Usuda M and Hamada N 2000 *J. Phys. Soc. Japan* **69** 744
- [24] Ueda K and Hosono H 2002 *Thin Solid Films* **411** 115
- [25] Czyżyk M T and Sawatzky G A 1994 *Phys. Rev. B* **49** 14211
- [26] Lang J K, Baer Y and Cox P A 1981 *J. Phys. F: Met. Phys.* **11** 121
- [27] Duò L, Finazzi M and Braicovich L 1993 *Phys. Rev. B* **48** 10728
- [28] Reihl B, Riesterer T, Bednorz J G and Müller K A 1987 *Phys. Rev.* **35** 8804
- [29] Gao Y, Wagener T J, Weaver J H, Arko A J, Flandermeier B and Capone D W II 1987 *Phys. Rev. B* **36** 3971
- [30] Shannon R D 1976 *Acta Crystallogr. A* **32** 751
- [31] Yeh J J 1993 *Atomic Calculation of Photoionization Cross-Sections and Asymmetry Parameters* (London: Gordon and Breach)